Available online at www.sciencedirect.com
ScienceDirect
Fuel 86 (2007) 1908–1917
FUEL
www.fuelfirst.com

Average structural analysis of the extractable material of young soot gathered in an ethylene inverse diffusion flame

Alexander Santamaría [a], Fanor Mondragón [a,*], Wiston Quiñónez [a], Eric G. Eddings [b], Adel F. Sarofim [b]

[a] *Institute of Chemistry, University of Antioquia, A.A. 1226, Medellín, Colombia*
[b] *Department of Chemical Engineering, University of Utah, Salt Lake City, UT 84112, USA*

Received 13 June 2006; received in revised form 18 November 2006; accepted 4 December 2006
Available online 2 January 2007

Abstract

Conventional analytical methods such as ^{1}H NMR, vapor pressure osmometry (VPO) and elemental analysis were used to characterize the soot precursor material represented by the chloroform extractable fractions of the young soot gathered at different heights of an ethylene inverse diffusion flame in terms of average structural parameters. The results indicate that the soot soluble fraction obtained at a 6 mm height has a relatively large molecular weight and has long aliphatic chains which later disappear with an increase in height above the burner base, especially in the region where the temperature is high (1200 K). This behavior is also accompanied by an increase in the aromaticity (f_a) of the samples.

Keywords: Soot; Nuclear magnetic resonance; Average structural parameters

1. Introduction

Soot formation during the incomplete combustion of hydrocarbons is an issue of practical importance. It demands a molecular-level understanding of soot forming processes and products of high molecular weight in order to develop new strategies that allow for control of emissions of particulate matter into the environment. Soot formation is a very complex phenomenon involving homogeneous and heterogeneous processes as well as competition among formation, oxidation and bond scission reactions [1–5]. Although the process of soot evolution has been investigated both experimentally and theoretically in many studies [1–22], there are still some questions that need to be addressed regarding the chemical structure of the different compounds formed in the flame, particularly during the early stages of soot formation that is commonly known as the soot inception stage.

The soot inception process has been the target of several research studies [3,5–9]. Nevertheless, the investigation in this area has been relatively limited in comparison with the studies that describe the global process of soot formation. With regard to intermediate products of soot particle formation, studies on reaction pathways and kinetics of PAH formation have made great progress [4,8]; however, the precursor particles resulting from PAH growth are still under study.

Previous studies performed in normal diffusion flames (NDF) identified the presence of soot precursor particles in combustion systems, using thermophoretic particle deposition on a cooled target that was placed by rapid insertion into the centerline of the flame [11–13]. However, the results of these studies were just limited to transmission electron microscopy (TEM) and laser microprobe mass spectrometry (LMMS) analyses, due to the small amount of sample that could be collected from the centerline of

* Corresponding author. Tel.: +57 4 210 6613; fax: +57 4 210 6565.
E-mail address: fmondra@quimbaya.udea.edu.co (F. Mondragón).

0016-2361/$ - see front matter © 2006 Elsevier Ltd. All rights reserved.
doi:10.1016/j.fuel.2006.12.002

the flame. Although these results made a significant contribution to understanding the chemistry and morphology of soot precursor particles, it is still a problem to collect a large amount of this material. In addition, one disadvantages of the LMMS technique is that it fails to detect aliphatic hydrocarbons and light aromatic compounds that are evaporated into the vacuum to which a sample is exposed [11–13]. Therefore, to overcome this difficulty, a new flame configuration was needed.

The inverse diffusion flame (IDF) appears to be a good alternative for studying the chemistry of the early stages of the soot formation process for the following reasons. The combustion products formed in the fuel side never enter to the oxidation zone and escape unoxidized from the flame[6,7,13–19] and the soot obtained in an IDF configuration is younger in nature and can be collected from the surroundings without the need to invade the flame with the sampling probe. In addition, soot collected from this type of flame possesses the characteristic of relatively high solubility in chloroform (more than 50%, depending on the sampling position), which allows use of a great variety of analytical techniques [7,19].

It has been shown that the soot inception process occurs through coagulation reactions of large polycyclic aromatic hydrocarbons (PAHs) [2,4,6,8,9]. It is also recognized that the growth mechanism of the primary particles occurs through carbon addition reactions (mainly C2) from the gaseous phase to the particle surface with later H_2 production. This process is currently described in a mechanistic model termed HACA (hydrogen abstraction acetylene addition) [2]. However, very little is known about the chemical structure of these compounds. In particular, the role is not clearly known for both the aliphatic component constituted by more than two carbon atoms and the oxygenated species observed in the condensed phase during the soot inception and growth processes [19,25,33].

In a study published by Ciajolo et al. [20,21], the soot extractable material obtained in the soot inception region of an ethylene premixed flame was chemically characterized using UV–vis and FT-IR analyses, and the results indicated that the extractable fraction of the soot demonstrated not only aromatic but also aliphatic characteristics, and these characteristics were observed both before and after the soot inception point. For example, at low flame positions just below the soot inception point, a significant contribution of aromatic hydrogen was observed and reached its maximum value at the inception point. However, after this point, the aromatic hydrogen contribution decreases, while the aliphatic hydrogen content due to both CH_2 and CH_3 groups were much more significant.

A quantitative analysis done by the same group using FT-IR indicated that for each CH_3 group there are at least five CH_2 groups present in the extractable material species [21]. Similar results were obtained by Oktem et al. [22], using mass spectrometry. The results indicated that the aliphatic component present in the semivolatile material has an important contribution in the soot growth process just after soot inception, or once the first particles have been formed.

Recently, in a study carried out in our laboratory using an ethylene inverse diffusion flame, an interesting trend was found along the flame that is opposite to the one observed in the premixed flames reported by Ciajolo and Oktem [19–22]. Our results [19] showed that the extractable material of soot obtained at low flame positions presented a significant content of aliphatic structures, which started disappearing as height above the burner increased as result of bond scission and cyclization reactions, and lead to the formation of more compact molecules with high aromatic character.

Although the trends in the results of our study were opposite to those reported in premixed flames, these results should be viewed as complementary given that the differences between soot formation in premixed flames, and IDFs lies in the time–temperature history and the spatial separation for the carbonization and oxidation processes. Therefore, it is expected that the intermediate hydrocarbons and soot produced in this flame should have a different evolution history as a function of height above the burner, as compared to a premixed flame. Although this information is very useful, a detailed description is still lacking of the chemical structure of the different compounds present in the extractable material of young soot.

In general, the soot soluble fraction in solvents is, as well as the soluble fractions of oil and coal, a complex mixture of hydrocarbons. Currently, several spectroscopic and separation techniques have been used to characterize those mixtures (mainly from oil and coal) in order to obtain a more detailed structural profile [23,24,26–32]. In particular, the proton and carbon nuclear magnetic resonance techniques have been useful to determine the structural skeleton of several fossil fuels [23–32]. Nevertheless, neither the NMR spectra, nor other spectroscopic and analytical data provides enough information to completely delineate the individual components of a mixture. Therefore, due to this complexity, and the necessity to represent the composition of these fractions in a systematic way, the concept of ''average structure'' has arisen. These structures are generally based on nuclear magnetic resonance information combined with elemental analysis and molecular weight [23,24,28]. The intent of this approach is to characterize a soluble fraction in a particular solvent using average structural parameters that later can be used to outline the possible average chemical structures.

Although this type of analysis has been routinely used to characterize liquid oil and coal liquid fractions [23–32], to the knowledge of the authors it has not been used to characterize the soot precursor material that is soluble in solvents. Therefore, the purpose of this study is to obtain chemical structure information of extractable material of soot gathered from an ethylene inverse diffusion flame through average structural parameters such as aliphatic chain length, number of fused aromatic rings, and number of substituents per aromatic cluster, etc., using conventional analytical techniques such as ^{1}H NMR, vapor pressure osmometry (VPO) and elemental analysis.

2. Experimental

2.1. Burner and sampling probe

The inverse diffusion flame burner (IDF) has been described in detail elsewhere [19]; however, this paper presents a brief description of the experimental setup (see Fig. 1). The burner consists of three concentric brass tubes: a central tube or air jet (11 mm); an intermediate tube (38 mm) used for supplying the fuel (ethylene), and an outer tube for a N_2 stream (75 mm) that is used as a shield to prevent the formation of flames with the room air. The flow conditions for the gaseous streams were 27, 117 and 289 cm^3/s for the air, fuel, and N_2, respectively, and the visible flame height which was established from the burner mouth to the flame visible tip was kept at 60 mm in all experiments.

Soot samples were taken at different heights (6, 15, 25, 30, 35, 45 mm and exhaust) along the lateral axis of an ethylene inverse diffusion flame using a 10 cm long stainless steel probe with a 1 mm I.D. capillary tip. Potential catalytic effects of the stainless steel probe were evaluated by comparison against samples taken with a quartz probe, and catalytic effects were found to be negligible. The stainless steel probe was thus used for experimental convenience.

The sampling probe was connected to a vacuum system in line with both a teflon filter and a cold trap used to gather the particulate matter and volatile compounds, respectively. The soot samples were subjected to extraction with chloroform in an ultrasonic bath for 15 min. Then, the solvent was evaporated in an inert atmosphere at room temperature and the extracts obtained were stored for later characterization.

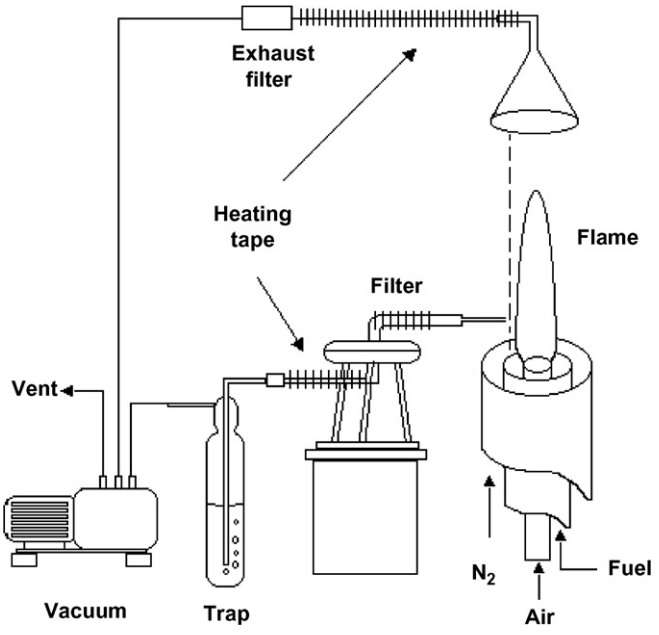

Fig. 1. Schematic representation of the IDF burner.

2.2. Flame temperature

The temperature profile at the flame sampling position was measured using an R type thermocouple (Pt–Pt 13% Rh, with 75 μm wire and with a bead diameter of about 150 μm), which was placed into the flame by a rapid insertion technique in order to reduce the thermocouple exposure time in sooting flame regions. The temperature information was recorded using a Labjack data acquisition system connected in line with an EI-1040 amplifier that provides high impedance and high gain. Radiation corrections due to heat losses were performed for the thermocouple readings in all the experiments.

2.3. ^1H NMR analysis

^1H NMR spectra were carried out on the chloroform extractable material of soot samples collected in the filter. For the ^1H NMR experiments, the extracts were re-dissolved in $CDCl_3$ containing a trace amount of tetramethylsilane (TMS), which was used as an internal chemical shift reference. All spectra were taken in a Bruker AMX 300 spectrometer equipped with a 5 mm inner diameter tube and operated at a frequency of 300 MHz.

Before starting the analysis, the spectra obtained were corrected for phase and baseline and then each of them was separated into seven typical regions that correspond to seven different protons (H_γ, $H_{\beta1}$, $H_{\beta2}$, H_α, H_f, H_o and H_a) according to their position in the molecule. Later, each spectrum was integrated within the indicated regions. See the corresponding ^1H NMR assignments in Refs. [19,29].

2.4. VPO measurements

Average molecular weight data of the extractable material of soot generated in the flame was determined by vapor pressure osmometry (VPO) in a Knauer osmometer using chloroform as solvent and benzyl as calibration standard. All measurements were carried out using sample and standard solutions of 1 g/kg and 0.00 5 mol/kg, respectively. Then, the average molecular weight (MW) was obtained from the K_{cal}/K_s ratio, where K_{cal} is the benzyl calibration constant expressed in kg/mol and K_s is the sample constant, which is expressed in kg/g. The minimum molecular weight that can be determined by this technique using organic solvents is about 40 g/mol.

2.5. Elemental analysis

The elemental analysis of the samples was carried out by the conventional combustion method using a Perkin–Elmer CHN analyzer. Oxygen content was obtained by difference.

3. Average structural parameters calculations

Some of the first studies that used ^1H NMR analysis to obtain average structural parameters in complex mixture of

hydrocarbons were published by William [31] and Brown and Ladner [32]. In these studies the authors reported a set of structural parameters such as aromaticity (f_a), substitution degree (σ), branching index (BI), and aromatic condensation index, which were used to describe some heavy oil fractions. Years later, Clutter et al. [24] extended the model implemented by the former authors by introducing ^{13}C NMR analysis in the interpretation of their results. Although nowadays there are much more precise models to describe complex mixtures of hydrocarbons, they are also much more complex and difficult to apply. Also, it is necessary to have a broad knowledge of the chemical composition of the sample [26,27].

Most of the parameters evaluated in the classic methods are generally extracted from hypothetical structural models and they present a simple calculation method that leads to a direct and rational interpretation of the results, which in turn present a significant semi-quantitative content [24,30–32]. Therefore, some parameters evaluated in previous works were modified and incorporated into our calculation model. These parameters were used to characterize the extractable material of soot obtained in an ethylene inverse diffusion flame and they are described in Table 1.

The equations used to calculate the average structural parameters are summarized in the Table 2. The variables $H^*_\gamma, H^*_{\beta1}, H^*_{\beta2}, H^*_\alpha, H^*_f, H^*_o$ and H^*_a, correspond to the molar fraction of the normalized integrals of the different types of hydrogen identified in the ^1H NMR spectra; whereas, the variables C^*, H^*, O^*, O^*_E, and O^*_q correspond to the molar fraction of carbon, hydrogen and total oxygen coming directly from elemental analysis. Note that the total oxygen content was divided in two components labeled with the letters q and E, which were assigned to benzoquinone–carbonyl and ether groups according to FT-IR analysis in Refs. [19,34,35].

Table 1
Average structural parameter definitions

C^*	Molar fraction of carbons obtained by elemental analysis
H^*	Molar fraction of hydrogen obtained by elemental analysis
O^*	Molar fraction of oxygen obtained by elemental analysis
MW	Average molecular weight of the samples
f_a	Fraction of carbons which are aromatic
f_{al}	Fraction of carbons which are aliphatic
$f_{\alpha,(f)}$	Fraction of α and (f) fluorene type carbons attached to aromatic rings
f_{aHa}	Fraction of aromatic carbons substituted by aromatic hydrogen
f_o	Fraction of carbon in olefinic groups
f_q	Fraction of carbon in carbonyl groups
$\%C_i$	Weight fraction of C_i carbon, with i = a, al, α, f…
$\#C_i$	Average number of C_i carbons per average structural unit, with i = a, al, α, f…
$\#O_i$	Average number of oxygen present in carbonyl groups ($i = q$) and ether groups ($i = E$). This calculation is based on elemental analysis only
$\#C^S_a$	Average number of aromatic carbons substituted by alkyl and oxygenated groups
$(C/H)^*_{al}$	C/H molar ratio in aliphatic groups
L	Chain length number per average structural unit
R_a	Number of fused aromatic rings per average structural unit

Table 2
Average structural parameter equations

$f_a = \frac{[C^* - (0.33H^*_\gamma + 0.4H^*_{\beta1} + 0.5(H^*_{\beta2} + H^*_\alpha + H^*_f) + H^*_o + C^*_q)]}{C^*}$	1
$f_{al} = \frac{[(0.33H^*_\gamma + 0.4H^*_{\beta1} + 0.5(H^*_{\beta2} + H^*_\alpha + H^*_f))]}{C^*}$	2
$f_{\alpha,(f)} = \frac{[0.5H^*_{\alpha,(f)}]}{C^*}$	3
$f_{aHa} = \frac{Ha^*}{C^*}$	4
$f_o = \frac{H^*_o}{C^*}$	5
$f_q = \frac{C^*_q}{C^*} = \frac{O^*_q}{C^*}$	6
$\%C_i = f_i(\%C) \quad i$ = a, al, α, f…	7
$\#C_i = (\%C_i)\mathrm{MW}/1200 \quad i$ = a, al, α, f…	8
$\#O_i = (\%O_i)\mathrm{MW}/1600 \quad i$ = q, E	9
$\left(\frac{C}{H}\right)^*_{al} = \frac{[(0.33H^*_\gamma + 0.4H^*_{\beta1} + 0.5(H^*_{\beta2} + H^*_\alpha + H^*_f))]}{(H^*_\gamma + H^*_{\beta1} + H^*_{\beta2} + H^*_\alpha + H^*_f)} \left(\frac{H}{C}\right)^*$	10
$L = (\#C_{al} - \#C_f)/\#C_\alpha$	11
$Ra = 1 + (\#C_a - \#C^s_a)/2$	12

In the derivation of the equations used in this study, several assumptions must be taken into account to determine these parameters. First, the alkyl and oxygenated groups present in the sample are attached directly to aromatic rings. Second, the aliphatic groups are mainly linear aliphatic chains, where the C/H = 0.33 ratio in γ position comes mainly from CH_3 groups; whereas, the C/H = 0.4 ratio in β1 position is an average value between CH_2 and CH_3 groups, respectively. In the remaining positions (α, β2, y, f) a C/H ratio of 0.5 is assumed. Nevertheless, this assumption breaks down when the branching degree of the aliphatic chains among samples increases. And third, the total oxygen content obtained by elemental analysis is assumed to be mainly distributed into two oxygenated species (carbonyl and ether type), and this observation has been previously corroborated in our laboratory by FT-IR analysis [19]. Some other authors have also identified the presence of oxygenated species in soot extracts coming from several sources using different analytical techniques. These results indicated that at least 50% of the total oxygen content is present in benzoquinone type carbonyl groups [34,35].

4. Results and discussion

One of the most important factors to keep in mind in a discussion about chemical transformations in combustion processes is the temperature. Fig. 2 shows the temperature profile at the sampling position that we are evaluating in this study, which is located along the lateral axis (6 mm from the centerline) of an ethylene inverse diffusion flame. Note that the temperature peak reached at about a 15 mm height does not surpass 1380 K. Prior to this point, the temperature is high, particularly close to the burner surface (1200 K), and then increases gradually until it reaches the maximum temperature peak. After passing this point, the

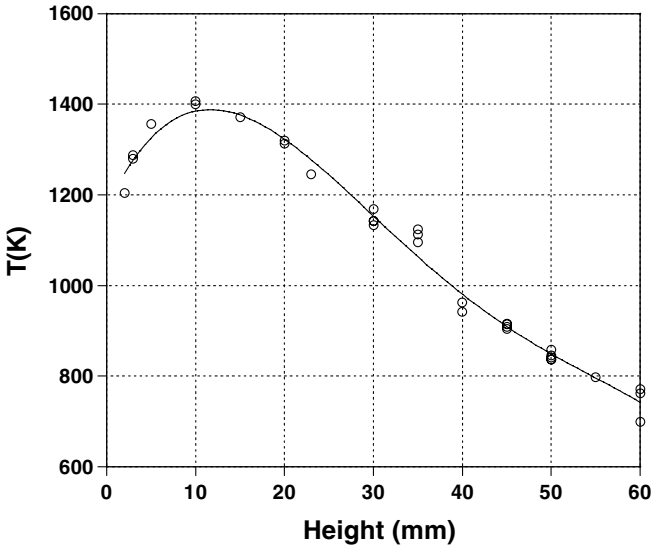

Fig. 2. Temperature profile of an ethylene inverse diffusion flame at the sampling position (6 mm from the centerline).

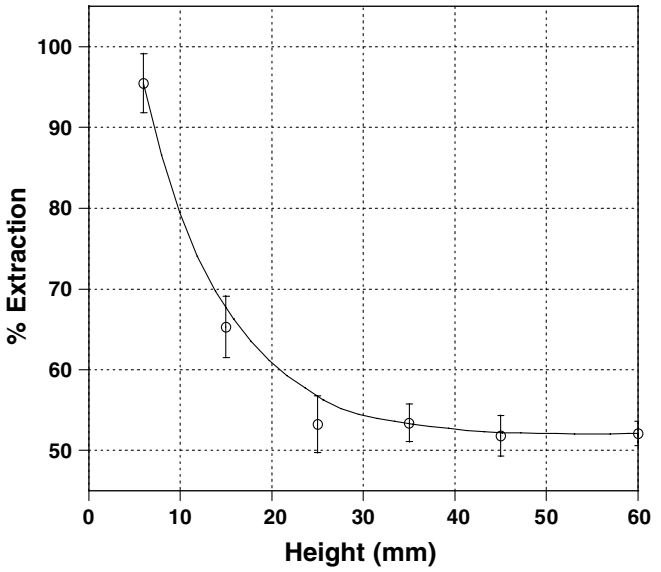

Fig. 3. Weight percentage of extractable material of soot gathered from an ethylene inverse diffusion flame.

temperature decreases rapidly up to 800 K just at the flame tip.

The sampling temperature of the inverse diffusion flame evaluated in our study is relatively high, as shown in Fig. 2, but not as high as the temperatures found at the centerline of premixed and normal diffusion flames. Thus, it is expected that the global oxidation–carbonization process experienced by the soot particles in an inverse diffusion flame should be less drastic as compared to its counterpart, since the time–temperature history for these processes is different. It is important, however, to highlight that the thermal decomposition taking place along the lateral axis of an inverse diffusion flame is reflected in a significant reduction of hydrogen content followed by an increase in the degree of aromatization of the samples as a function of height as was observed in our previous paper [19]. This observation implies that bond scissions, cyclization, and isomerization reactions among the chemical species formed in the flame can be favored, particularly, during the first 40 mm, where the temperature is sufficiently high.

The increment in the degree of aromaticity mentioned previously is also reflected in the low solubility of the samples in chloroform observed as a function of height. Fig. 3 shows the weight percentage variation of soot extractable material as a function of height. It is observed that at positions closer to the burner face, the amount of extractable material increases. For instance, the sample taken at 6 mm is about a 95% extractable in chloroform, with the remaining 5% of the sample corresponding to a carbonaceous solid material which is highly condensed and insoluble in chloroform. At this point in the flame we have gaseous species, which are not the object of the present work, plus a tarry material identified as a precursor to soot particles. The carbonaceous particles themselves are just forming at this point (possibly earlier), but their concentration is still low. However, after a 6 mm height, the amount of extractable material of soot samples decreases until it reaches a constant value (≈51%) that is observed in all the samples taken over 35 mm. This value is in good agreement with values reported in the scientific literature for the solubility of young soot gathered at the exhaust of an ethylene inverse diffusion flame [7,19].

The average molecular weight obtained by VPO shows a similar behavior to that observed in the solubility profile, since the sample taken at the lowest flame position shows the highest average molecular weight among the samples evaluated (MW = 817, see Table 3). The table also shows that the average molecular weight diminishes with height up to reaching a constant value after 35 mm, which also indicates that the average chemical structure must be very similar among these samples.

The high molecular weight observed in the samples taken at 6 mm and 15 mm is mainly due to the high contribution of oxygen and aliphatic structures present in these samples. It is important to note that aromatic clusters are quickly formed in the flame as indicated by the average structural analysis that we are going to see further on. An analysis done by Mikosfki [36] showed that polycyclic

Table 3
Elemental analysis and average molecular weight of the soot extractable material

Sampling height (mm)	%C	%H	%O	(C/H) Total	MW
6.0	85.3	7.71	7.02	0.92	817
15.0	86.5	6.42	7.12	1.12	628
25.0	88.9	5.44	5.67	1.36	356
35.0	90.2	4.90	4.90	1.53	335
45.0	92.9	4.89	2.21	1.58	326
60.0	93.6	5.24	1.12	1.49	331
Exhaust	93.7	5.20	1.12	1.50	413

aromatic hydrocarbon (PAH) formation in an ethylene inverse diffusion flame takes place rapidly close to the burner surface, which is consistent with our results.

The elemental analysis showed that the soot precursor material gathered in an ethylene inverse diffusion flame consists basically of C, H, and O (see Table 3). The carbon content of the chloroform soluble products taken between 6 mm and the exhaust increases from 85% to 95%, accompanied by a corresponding reduction in the hydrogen content, which changes from 8% to 5%. A detailed analysis shows that the total (C/H) ratio increases significantly with height, particularly during the first 35 mm, which implies that the aromatic character and degree of condensation of these samples increase. Nevertheless, after this point the total (C/H) ratio reaches a constant value of about 1.50, which indicates that the samples present a very similar chemical composition. Similar values of total (C/H) ratio have been found in the literature for soot particle precursors obtained in ethylene premixed flames [7,21].

Dobbins et al. [10,12] characterized soot precursor particles and carbonaceous soot taken at the centerline of an ethylene NDF using LMMS. Based on this analytical technique, they reported C/H ratios of 1.8 for precursor particles obtained lower in the flame, and 5.6 for carbonaceous soot obtained higher up in the flame. The former value is consistent with the C/H ratio reported by Blevins et al. [7] for soot precursor particles obtained at the exhaust of an ethylene IDF, and precursor particles obtained in this work above 35 mm. However, at low flame positions in the IDF the C/H indicates that the soot precursor particles generated in this range of heights are even younger.

Another important characteristic observed in the elemental analysis is that all the extracts of soot samples taken at low flame positions (below 35 mm) showed a significant oxygen content, which decreases gradually with height from 7% to 5%. However, after 35 mm the oxygen content in the samples falls down to 1%, value that remains constant even in the sample taken at the exhaust.

FT-IR analysis described in reference [19] confirmed the presence of oxygenated functional groups in these samples; most of the signals correspond to C=O stretching of carbonyl groups (1720 cm^{-1}) and C–O–C stretching of ether groups (1000–1300 cm^{-1}). Although several authors have reported the presence of oxygenated functional groups in soot samples, its origin is not very clear [19,25,33–35]. The present results show a clear trend with height along the flame, which suggests that this group of compounds may be involved in the normal soot formation process. Nevertheless we cannot discard the possibility that the oxygen has been added during the sampling process. Unfortunately, this type of potential artifact is difficult to eliminate since the separation of oxidation and carbonization processes at the sampling position evaluated in this study is much more difficult to achieve.

Fig. 4, shows the ^{1}H NMR spectrum of the soot extractable fraction taken close to the burner base (6 mm). In the same figure, it is possible to observe the classification of the different types of hydrogen. The main assigned groups correspond to: hydrogen on aromatic rings (H_a), olefinic hydrogen (H_o), hydrogen on carbon connecting two aromatic units or fluorene type (H_f), hydrogen of CH, CH_2 and CH_3 groups on α position to aromatic rings (H_α), hydrogen of CH_2 groups (naphthenic type) on β position to aromatic rings ($H_{\beta1}$), hydrogen of CH, CH_2 and CH_3 groups on β position to aromatic rings ($H_{\beta2}$), and hydrogen of terminal methyl groups on γ, δ or greater positions to aromatic rings.

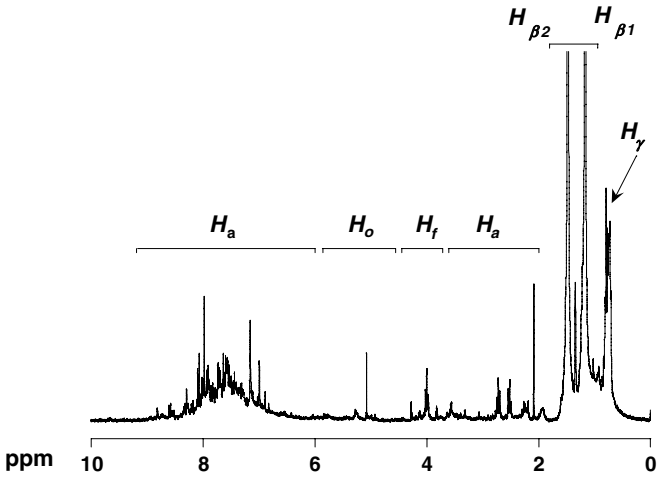

Fig. 4. ^{1}H NMR spectrum of the extractable material of soot taken at 6 mm from the flame.

It is worth highlighting that the integration limits for the hydrogens that belong to CH, CH_2 and CH_3 groups in a determined region of the spectrum are not easy to establish due to a high degree of signal overlapping. Nevertheless, taking as a guide the classification done by Guillén et al. [29], which was obtained from a blend of model compounds, the cut points in the spectra could be identified with much more precision and the range of the different hydrogen groups could be determined in this way and subsequently taken into account in our work.

Fig. 5 shows the ^{1}H NMR spectra of samples evaluated in this study. In general, the samples taken at low flame positions (below 35 mm) present a significant aliphatic contribution, particularly in the sample taken close to the burner base, where the aliphatic content corresponds to about 60% of total hydrogen of the sample. Even so, as the height above the burner increases, the aliphatic character decreases, which is reflected as well in the reduction of the hydrogen content H_γ, $H_{\beta1}$, and $H_{\beta2}$, respectively (see Table 4). This behavior is also followed by an increase in the aromatic character of the samples, with the highest values found in the extractable fraction of soot taken at the exhaust.

Table 4 shows the weight percent distribution of the different hydrogen types observed by ^{1}H NMR, calculated based on the total hydrogen content obtained by elemental analysis. This table shows that the aliphatic hydrogen con-

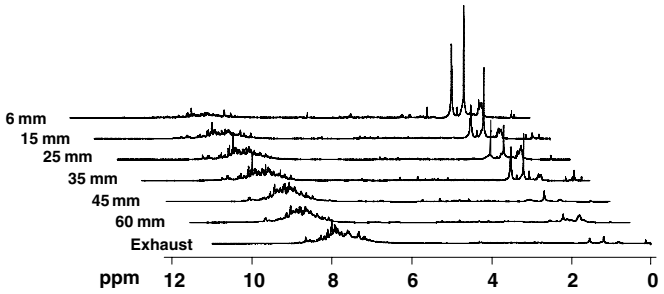

Fig. 5. ^{1}H NMR spectra of the extractable material as a function of height above the burner surface.

Table 4
Weight percent distribution of the hydrogen observed by ^{1}H NMR

Sampling height (mm)	$\%H_\gamma$	$\%H_{\beta1}$	$\%H_{\beta2}$	$\%H_\alpha$	$\%H_f$	$\%H_o$	$\%H_a$
6.0	1.01	1.95	1.60	0.79	0.25	0.29	1.82
15.0	0.52	1.08	0.87	0.52	0.22	0.20	3.01
25.0	0.46	0.68	0.42	0.18	0.094	0.072	3.52
35.0	0.34	0.53	0.34	0.15	0.067	0.065	3.41
45.0	0.25	0.20	0.14	0.18	0.065	0.060	3.99
60.0	0.18	0.27	0.14	0.16	0.056	0.038	4.39
Exhaust	0.094	0.25	0.16	0.14	0.04	0.035	4.49

tent corresponding to methyl and methylene groups ($H_{\beta1}$ and $H_{\beta2}$) suffer the most drastic reduction among the hydrogens observed in this study. For example, the sum of the hydrogen $H_{\beta1}$ and $H_{\beta2}$ for the sample obtained at 6 mm corresponds to nearly 50% of the total hydrogen content, whereas the $H_{\beta1}$ and $H_{\beta2}$ content for the sample at the exhaust reaches only 10%. Also, it is important to observe that the extractable material of the soot sample taken at 6 mm shows a significant hydrogen contribution at the γ position that corresponds mainly to methyl terminal groups on aliphatic chains, an observation that suggests the existence of large aliphatic chains, which would also be associated with the high content of β hydrogen observed. As was mentioned in the introduction, Ciajolo and Oktem [20–22] have observed that the aliphatic structures present in the extractable material significantly contribute to soot mass growth after the soot inception point. The same observation may be applicable to the soot samples taken at low positions in our flame, since we are already sampling a few millimeters after the soot inception point.

The remainder of the alkyl hydrogen groups observed in the spectra present a less significant, but equally important contribution. For example, the hydrogen content on the α position to aromatic rings gives us an idea of the degree of aromatic substitution. Table 4 shows that the degree of aromatic substitution among the samples decreases as height above the burner increases. This means that the sample taken at the exhaust consists basically of a condensed aromatic nucleus only, an observation that is reflected in an increase of the aromatic hydrogen content of this sample, which corresponds to 87% of the total hydrogen. On the other hand, the hydrogen fractions H_f and H_o show an apparent contribution at slightly lower flame positions, where the possibility exists of finding at least a fluorene type bridge and an olefinic group per average structural unit.

In this study, some average structural parameters were calculated based on the hydrogen content obtained by ^{1}H NMR and elemental analysis. Three replicates were carried out on each pair of samples so that the precision of the method could be estimated. The parameters fall into three categories according to the estimated precision: (1) parameters with an error <5%; f_a, f_f, R_a; (2) parameters with 5% < error < 10%; f_{al}, f_{aHa}, f_o, and (3) parameters with 10% < error < 20%; f_α and L. Similarly, other parameters associated with those previously described, such as $\%C_i$ and $\#C_i$ (con i = a, al, f...), are also included into the assigned categories.

In particular, the parameter associated with the degree of aliphatic substitution (f_α) is quite variable among the samples and the error involved is relatively high, and this error is also reflected in the average chain length calculation (L). Thus, the parameters f_α and L should therefore be considered as estimates.

The results of these calculations are summarized in Table 5, where several features are observed. The fraction of aromatic carbon or aromaticity of the samples (f_a) evaluated in this study increases from 0.59 to 0.96 as height above the burner increases, which corresponds to an increase in the weight percentage from 49% to 89.5%. A similar pattern is observed after analysis of the fraction of aromatic carbons substituted by aromatic hydrogen (f_{aHa}), but in this case, the weight percentage associated with this fraction is lower and changes with height between 22% and 56%. This result means that at least half of the

Table 5
Average structural parameters results

Parameter	Sampling height above the burner (mm)						
	6	15	25	35	45	60	Exhaust
f_a	0.59	0.75	0.86	0.89	0.95	0.95	0.96
f_{al}	0.34	0.20	0.11	0.08	0.05	0.05	0.04
f_α	0.06	0.04	0.01	0.01	0.01	0.01	0.01
f_{aHa}	0.26	0.42	0.48	0.45	0.52	0.56	0.60
$\%C_a$	49.9	64.5	76.6	80.4	87.9	88.9	89.5
$\%C_{al}$	29.3	16.9	9.3	7.2	4.3	4.3	3.7
$\%C_\alpha$	4.74	3.12	1.14	0.89	1.07	0.98	0.86
$\%C_{aHa}$	21.8	36.1	42.2	40.9	47.9	52.6	55.9
$\#C_a$	34.0	33.7	22.7	22.4	23.9	24.5	30.8
$\#C_{al}$	19.9	8.9	2.8	2.0	1.2	1.2	1.3
$\#C_\alpha$	3.23	1.6	0.34	0.25	0.30	0.27	0.30
$\#C_\alpha$ (fitted)	3.0	2.0	1.0	1.0	1.0	1.0	1.0
$\#C_f$	1.04	0.69	0.17	0.11	0.11	0.09	0.08
$\#C_o$	2.34	1.26	0.26	0.22	0.20	0.13	0.15
$\#C_{aHa}$	14.9	18.9	12.5	11.4	13.0	14.5	19.2
$\#C_q$	1.79	1.40	0.63	0.51	0.00	0.00	0.00
$\#O_E$	1.79	1.40	0.63	0.51	0.45	0.23	0.29
L	6.30	4.08	2.60	1.91	1.06	1.08	1.20
R_a	5.07	4.70	4.66	5.28	5.50	5.23	5.97
C/H_{al}	0.47	0.39	0.31	0.28	0.27	0.29	0.29

total amount of aromatic carbons present in the samples is involved in fused aromatic rings and in the substitution by alkyl groups.

The aliphatic component describes a completely opposite behavior. Table 5 shows that the fraction of aliphatic carbons (f_{al}) decreases from 0.34 for the sample taken at 6 mm to 0.04 for the sample taken at the exhaust, and these values correspond to a change in the weight percentage of total carbon from 29.3% to 3.7%, respectively.

Similarly, it is possible to observe from these results that the aliphatic contribution is important at lower flame positions, but after 35 mm, the fraction of aliphatic carbons reaches a constant value. This result can be also confirmed through the aliphatic carbon–hydrogen ratio $(C/H)_{al}$.

Another quite important parameter that is related to the degree of aliphatic substitution is the fraction of carbons on α position to aromatic rings, described as f_α. Because this fraction contributes to the aliphatic component, its behavior is similar and decreases as height increases. Therefore, it is expected that the number of substituents and the chain length should be greater in the samples taken at positions closer to the burner face since the aliphatic carbon fraction is also greater. Unfortunately, the error associated with this parameter can be relatively high, which leads to an underestimation in the α carbon number ($\#C_\alpha$), which also affects the average chain length calculation (L). However, quite a good approximation can be made if the aliphatic carbon number ($\#C_{al}$) present in the samples is taken into account. For example, samples taken after 35 mm have at least one aliphatic carbon atom on average with the possibility that it will be a CH_3 group joined directly to an aromatic ring. Thus, if we assume that all the aliphatic carbons of these samples are carbons on α positions, we can estimate the average chain length (L) in a much more precise way using Eq. (11) (Table 2).

Returning to the parameters associated with the aromatic carbon content, it is also possible to estimate the average number of fused aromatic rings per structural unit (R_a) using Eq. (12) (Table 2). Note that the numerator on the right hand of Eq. (12) (Table 2) $(\#C_a - \#C_a^S)$, corresponds to the total number of aromatic carbons that are fused in rings, which is obtained by subtracting the number of substituted aromatic carbons $(\#C_a^S)$ from the total number of aromatic carbons ($\#C_a$). The number $(\#C_a^S)$ is calculated from parameters such as: $\#C_{aHa}$, $\#C_\alpha$, $\#C_f$, and $\#C_o$. In addition, parameters corresponding to oxygenated species such as $\#C_q$ and $\#O_E$, were also included in this calculation.

The calculation results of L and R_a are summarized in Fig. 6. Note that at the lowest flame position (6 mm), the contribution of aliphatic structures is quite significant. Since the total number of aliphatic carbon atoms ($\#C_a$) for this sample is about 20 (see Table 5), there are at least 3 aliphatic chains per average structural unit, each one of them comprised of 6 carbon atoms. Then, the average number of carbons per aliphatic chain decreases rapidly during the first 35 mm, due to thermal decomposition processes caused by the high temperature of the system, which can favor the bond scission and cyclization reactions leading to the formation of highly condensed structures, as confirmed by the increment in the average number of fused aromatic rings R_a (5–6 rings per cluster). This result is also in good agreement with some GC–MS results reported in the literature where there have been identified significant concentrations of aromatic clusters between 4 and 7 rings assigned to pyrene and coronene, respectively [7]. Also, it is important to note that at low flame positions, the aromatic cluster is already quite large, which means that its formation takes place very early in the flame.

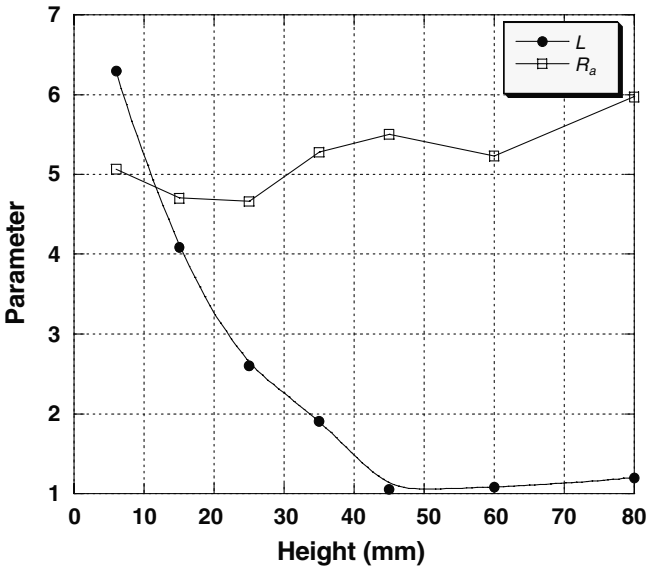

Fig. 6. Variation on chain length (L) and number of fused aromatic rigs (R_a) parameters as function of height.

Additionally, some structural parameters show a special feature since they strongly depend on the average molecular weight (MW). For example, the average number of aromatic carbons ($\#C_a$) and aromatic carbons substituted by aromatic hydrogen ($\#C_{aHa}$) per structural unit is larger in the samples that had higher molecular weight, that is, in the samples taken at 6 mm, 15 mm and the exhaust, respectively. Moreover, the parameters ($\#C_{al}$), ($\#C_\alpha$) and ($\#C_o$) do not have that dependency and the trend is much clearer indicating that the average number of these carbons decreases as height above the burner increases.

The results of this study provide an extension of the generalized chemical characterization of soot precursor material in our previous work using FT-IR and ^{1}H NMR [19]. In this work, we have introduced a new tool to chemically describe the soot precursor material obtained in an IDF through average structural parameters. This information can be used in conjunction with kinetic modeling studies to provide greater understanding of the soot inception process, which is one of less understood steps in soot formation due to the fast transformations that take place in the flame. In addition, the calculated average structural parameters in this study provide useful comparisons

between samples, which in turn can be used as a guide in the study of different processes including the use of additives.

5. Conclusions

The average structural analysis of soot precursor material indicates that in the initial stage of soot formation (6 mm), the sample is very aliphatic, with a high average molecular weight. In this case, 30% of the material is contained in aliphatic chains. Each structural unit has three aliphatic chains on average, each one composed of 6 carbon atoms. The average molecular weight per structural unit is reduced to almost half between the sample obtained at a height of 6 mm and the sample taken at the exhaust. This reduction is mainly due to the loss of aliphatic structures, which is also reflected in the reduction of the chain length (L) and the $(C/H)_{al}$ ratio. This behavior may be primarily due to thermal decomposition processes, since the temperature at low flame positions (below 35 mm) is fairly high; therefore, bond scission and some cyclization reactions are more frequent and leave behind a simple aromatic nucleus in which most of the carbon atoms are aromatic (89.5%).

On the other hand, the amount of soot extractable material in chloroform diminishes from 95% to 50%; therefore, it is necessary to consider coagulation reactions or fusion among structural units that lead to the formation of more compact and insoluble compounds in chloroform. This behavior is also corroborated through the average number of fused aromatic rings (R_a) which increases as height above the burner increases. An important feature that can be observed from these results is that the aromatic cluster is formed very early in the flame (6 mm) and consists of about 5 aromatic rings on average. Furthermore, it shows a high content of aliphatic structures and oxygenated species that favor the solubility of the sample and explain the high molecular weight observed.

Acknowledgements

The authors would like to thank the University of Antioquia for the support given to this project under the Sostenibilidad Program. A. Santamaria thanks Colciencias and the University of Antioquia for the Ph.D scholarship.

References

[1] Haynes BS. Soot and hydrocarbon combustion. In: Bartok W, Sarofim AF, editors. Fossil fuel combustion: a source book. New York: Wiley; 1991. p. 261–326.
[2] Frenklach M. Reaction mechanism of soot formation in flames. Phys Chem Chem Phys 2002;4(11):2028–37.
[3] Kennedy IM. Models of soot formation and oxidization. Prog Energy Combust Sci 1997;23:95–132.
[4] Richter H, Howard JB. Formation of polycyclic aromatic hydrocarbons and their growth to soot – a review of chemical reaction pathways. Prog Energy Combust Sci 2000;26:565–608.
[5] Glassman I. Soot formation in combustion process. Proc Combust Inst 1988;22:295–311.
[6] Katta VR, Blevins LG, Roquemore WM. Dynamics of an inverse diffusion flame and its role in polycyclic-aromatic-hydrocarbon and soot formation. Combust Flame 2005;142(1–2):33–51.
[7] Blevins LG, Fletcher RA, Benner BA, Steel EB, Mulholland GW. The existence of young soot in the exhaust of inverse diffusion flames. Proc Combust Inst 2002;29:2325–33.
[8] Violi A. Modeling of soot particle inception in aromatic and aliphatic premixed flames. Combust Flame 2004;139:279–87.
[9] Violi A, Sarofim AF, Truong TN. Quantum mechanical study of molecular weight growth process by combination of aromatic molecules. Combust Flame 2001;126:1506–15.
[10] Dobbins RA, Fletcher RS, Chang HC. The evolution of soot precursor particles in a diffusion flame. Combust Flame 1998;115:285–98.
[11] Dobbins RA, Megaridis CM. Morphology of flame-generated soot as determined by thermophoretic sampling. Langmuir 1987;3:254–9.
[12] Dobbins RA, Fletcher RA, Lu W. Laser-microprobe analysis of soot precursor particles and carbonaceous soot. Combust Flame 1995;100:301–10.
[13] Kaplan CR, Kailasanath K. Flow-field effects on soot formation in normal and inverse methane–air diffusion flames. Combust Flame 2001;124(1–2):275–94.
[14] Makel DB, Kennedy IM. Soot formation in laminar inverse diffusion flames. Combust Sci Technol 1994;97(4–6):303–14.
[15] Sidebotham GW, Glassman I. Flame temperature, fuel structure, and fuel concentration effects on soot formation in inverse diffusion flames. Combust Flame 1992;90:269–83.
[16] Sidebotham GW, Glassman I. Effect of oxygen addition to a near-sooting ethene inverse diffusion flame. Combust Sci Technol 1992;8:207–19.
[17] Wu KT, Essenhigh RH. Mapping and structure of inverse diffusion flames of methane. Proc Combust Inst 1984;20:1925–32.
[18] Oh KC, Lee UD, Shin HD, Lee EJ. The evolution of incipient soot particles in an inverse diffusion flame of ethane. Combust Flame 2005;140(3):249–54.
[19] Santamaria A, Mondragon F, Molina A, Eddings EG, Marsh ND, Sarofim AF. FT-IR and ^{1}H NMR Characterization of the products of an ethylene inverse diffusion flame. Combust Flame 2006;146(1–2):52–62.
[20] Ciajolo A, Barbella R, Tregrossi A, Bonfanti L. Spectroscopic and compositional signatures of PAH-loaded mixtures in the soot inception region of a premixed ethylene flame. Proc Combust Inst 1998;27:1481–7.
[21] Ciajolo A, Apicella B, Barbella R, Tregrossi A. Correlations of the spectroscopic properties with the chemical composition of the flame-formed aromatic mixtures. Combust Sci Technol 2000;153:19–32.
[22] Öktem B, Tolocka MP, Zhao B, Wang H, Johnston MV. Role of aliphatic and aromatic hydrocarbons in soot nucleation and growth in a laminar premixed ethylene–oxygen–argon flame. Combust Flame 2005;142:364–73.
[23] Lee SW, Glavincevski B. NMR method for determination of aromatics in middle distillate oils. Fuel Proc Technol 1999;60(1):81–6.
[24] Clutter DR, Petrakis LZ, Stenger RL, Jensen RK. Carbon-13 and proton nuclear magnetic resonance characterizations in terms of average molecule parameters. Anal Chem 1972;44(8):1395–405.
[25] Yan S, Jiang YJ, Marsh ND, Eddings EG, Sarofim AF, Pugmire RJ. Study of the evolution of soot from different fuels. Energy Fuel 2005;19:1804–11.
[26] Patrakov YF, Kamyanov VF, Fedyaeva ON. A structural model of the organic matter of Barzas liptobiolith coal. Fuel 2005;84(2–3):189–199.
[27] Yang Y, Liu B, Xi H, Sun X, Zhang T. Study on relationship between the concentration of hydrocarbon groups in heavy oils and their structural parameter from ^{1}H NMR spectra. Fuel 2003;82:721–7.
[28] Satou M, Nemoto H, Yokoyama S, Sanada Y. Determination of atomic groups of hydrocarbons in coal-derived liquids by high

performance liquid chromatography and nuclear magnetic resonance. Energy Fuel 1991;5:632–7.
[29] Guillen MD, Diaz C, Blanco CG. Characterization of coal tar pitches with different softening points by ^{1}H NMR; Role of the different kind of protons in thermal process. Fuel Proc Technol 1998;58:1–15.
[30] Cantor DM. Nuclear magnetic resonance spectrometric determination of average molecular structure parameters for coal-derived liquids. Anal Chem 1978;50(8):1185–7.
[31] Williams RB. Characterization of hydrocarbons in petroleum by nuclear magnetic resonance spectrometry. ASTM Spectrosc Technol Publ 1958;224:168–94.
[32] Brown JK, Ladner WR. A study of the hydrogen distribution in coal-like materials by high-resolution nuclear magnetic resonance spectroscopy II – a comparison with infrared measurement and the conversion to carbon structure. Fuel 1960;39:87–96.
[33] McKinnon JT, Meyer E, Howard JB. Infrared analysis of flame-generated PAH samples. Combust Flame 1996;105:161–6.
[34] Di Stasio S, Braun A. Comparative NEXAFS study in soot obtained from an ethylene/air flame, a diesel engine and graphite. Energy Fuel 2006;20(1):187–94.
[35] Kirchner U, Scheer V, Vogt R. FTIR spectroscopic investigation of the mechanism and kinetics of the heterogeneous reactions of NO_2 and HNO_3 with soot. J Phys Chem A 2000;104:8908–15.
[36] Mikofski MA. Flame structure and soot formation in inverse diffusion flames. University of California, CA USA, Berkeley, PhD thesis, 2005.